Bažant, Z.P., and Kim, Jang-Jay (1999). "Size effect in penetration fracture of sea ice plate: Review of theory and experimental evidence." *Ice in Surface Waters* (Proc., 14th Intern. Symp. on Ice, Clarkson College, Potsdam, NY, July 1998), H. T. Shen, Ed., Vol. 2, 1011–1018.

PROCEEDINGS OF THE 14TH INTERNATIONAL SYMPOSIUM ON ICE
POTSDAM/NEW YORK/USA/27-31 JULY 1998

Ice in Surface Waters

Edited by

Hung Tao Shen
Clarkson University, Potsdam, New York, USA

VOLUME 2

A.A.BALKEMA/ROTTERDAM/BROOKFIELD/1999

Ice in Surface Waters, Shen (ed.) © 1999 Balkema, Rotterdam, ISBN 90 5410 971 8

Size effect in penetration fracture of sea ice plate: Review of theory and experimental evidence

Zdeněk P. Bažant & Jang-Jay Kim
Department of Civil Engineering, Northwestern University, Evanston, Ill., USA

ABSTRACT: Vertical load capacity of a floating sea ice plate is analyzed by fracture mechanics. The radial bending cracks, which are considered to reach only through a part of the plate thickness and have a variable depth profile, are assumed to follow the Rice-Levy nonlinear softening line spring model. The plate-crack interaction is characterized in terms of the compliance functions for the plate wedge between radial cracks. Numerical calculations show a typical quasibrittle size effect such that the plot of $\log \sigma_N$ vs. $\log h$ (σ_N = nominal stress at maximum load, h = plate thickness) is a descending curve whose slope is negligible only for $h < 0.2$ m and then gets gradually steeper, asymptotically approaching $-1/2$. The calculated size effect agrees with the existing test data, and contradicts Sodhi's plasticity solution.

1 INTRODUCTION

In the early studies (Bernstein 1929, Nevel 1958), the load capacity of a floating sea ice plate was estimated on the basis of the tensile strength or yield criteria. Although much has subsequently been learned (Bernstein, 1929; Frankenstein, 1963; Kerr, 1975, 1996; Sodhi 1995a,b), the applicability of fracture mechanics has been doubted because laboratory tests indicate the notch sensitivity and size effect to be negligible. However, Dempsey (1989, 1990; also DeFranco and Dempsey 1990) showed this interpretation to be due to insufficient sizes of laboratory specimens in regard to the characteristic length of a quasibrittle material. The applicability of fracture mechanics on the large scale has recently been demonstrated by the in-situ experiments of Dempsey et al. (1995, 1996; also Adamson et al. 1995, Mulmule et al. 1995). The fact that the load-deflection curves of sea ice specimens exhibit postpeak softening rather than a plastic yield plateau implies, as a matter of principle, that fracture mechanics ought to be used and a size effect due to energy release ought to be expected (Bažant 1984; Bažant and Kim 1985; Bažant and Gettu 1991, Bažant and Chen 1997; Bažant and Planas 1998). The size effect is not statistical, nor fractal (Bažant and Planas 1998; Bažant 1997b).

Linear elastic fracture mechanics (LEFM) with full-through cracks was applied by Slepyan (1990), Bažant (1992a,b), Bažant and Li (1994a,b) and Li and Bažant (1994) to analyze the load capacity of sea ice with bending cracks. Bažant, Kim and Li (1995) and Dempsey et al. (1995) considered part-through cracks, and the former also the strength limit in the sense of cohesive cracks. Part-through cracks, documented in the field observations of Frankenstein (1963), transmit in-plane compressive forces and engender a dome effect which helps to carry the vertical load.

The objective of this paper is twofold: (1) to sketch a numerical solution by means of a system of integral equations based on the compliance functions of the floating plate wedge formed by two adjacent cracks and on Rice and Levy's model for part-through crack, as initially proposed by Bažant, Kim and Li (1995), and (2) to briefly discuss the numerical results and their significance for size effect. The detailed solution method and analysis of numerical results will be presented in a forthcoming journal article (Bažant and Kim 1998).

2 FRACTURE ANALYSIS

The floating ice plate, treated as an infinite elastic plate of thickness h, floats on water of specific weight ρ (Fig. 1) representing a Winkler elastic foundation. The differential equation for deflections w of the ice plate is $D\nabla^4 w + \rho w = 0$ where D = cylindrical stiffness of the plate. For the sake of simplicity, the plate is assumed to have a small circular

hole of a diameter roughly equal to the size of the penetrating object. The vertical load is applied uniformly along the edge of the plate. As confirmed by experiments as well as numerical calculations, radial cracks propagate in a star pattern. The plate wedges between the cracks may be assumed to be identical. The maximum load is known to occur when circumferential cracks initiate from the faces of the radial cracks.

The applications of fracture mechanics to this problem initially assumed the cracks to be full-through bending cracks. Their angles were at first assumed to be infinitely small (Bažant and Li 1994a,b), which allowed an analytical solution, and later to be finite, which required numerical analysis and was handled by finite difference energy minimization approach (Li and Bažant 1995). Subsequently, however, it was noted (Bažant et al. 1995) that the cracks reach through only a part of the plate thickness (Fig. 1) because the plate wedge prevents the faces of the crack from moving freely apart. So an in-plane compression force across the crack plane, shifted above the mid-thickness of plate, must develop. This engenders a dome effect, which helps carrying the load. This was ignored in previous solutions except Dempsey et al.'s (1995) in which, however, the crack depth was assumed to be uniform to allow an analytical solution. In reality, the crack depth varies significantly.

To solve the problem numerically, the vertical cracked cross section of the plate is subdivided into narrow vertical strips, in each of which the crack is assumed to propagate vertically. This simplification requires introducing a strength criterion for the initiation of the crack from the bottom surface, which means that the crack starts as a cohesive crack. The vertical growth of the crack is considered to follow LEFM and is modeled in terms of a distributed nonlinear softening line spring, as proposed by Rice and Levy (1972) and Okamura et al. (1972) (also Kuo et al. 1995). In each strip, the crack grows vertically as a function of the bending moment and normal force in the same strip only. The line spring model leads to the relations:

$$\Delta = \lambda_{11}.N + \lambda_{12}.M, \qquad \theta = \lambda_{21}.N + \lambda_{22}.M \tag{1}$$

where Δ, θ = additional in-plane circumferential relative displacement and relative rotation that are caused by the part-through crack (Fig. 1) and are conjugate to bending moment M and normal force N; λ_{ij} $(i,j = 1,2)$ = crack compliances, depending on crack depth b. Those for λ_{11} and λ_{22} are available in handbooks and λ_{12} was integrated from the known stress intensity factors.

The condition of compatibility with the plate wedge requires that the additional relative rotation θ and horizontal displacement Δ caused by the cracks be equal to the rotation and displacement calculated from the compliances of the plate wedge with respect to the nodes along the crack rays. The matrix of these compliances has been calculated numerically by finite difference energy minimization. The load-point displacement u is related by another elastic compliance matrix to load P and M and N in the strips.

Five stages of the vertical crack evolution in each strip are distinguished (Fig. 1). In stage 1, there is no crack as yet. In stage 2, the tensile strength limit is reached and the cohesive crack of depth b is assumed to be deform plastically, the flow rule being such that the ratio of plastic increments of rotation and normal strain at mid-thickness be the same as predicted by LEFM. In stage 3, there is a crack (of depth b). The aforementioned choice of the flow rule guarantees the bending moment and normal force to change continuously at the transition from stage 2 to stage 3 (this would not be the case if the plastic normality rule were assumed, and mixed stages 2 and 3 would then have to be considered). Stage 4, in which the cracked cross section is unloading elastically, and stage 5 in which the crack has closed, have also been programmed but never occurred for monotonic loading.

In a discretization with n strips along the radial ray, there are $3n+1$ unknown variables—the values of M, N and crack depths b in the strips, and the vertical load P. The remaining equations are provided by the crack propagation conditions (plastic or LEFM). Step-by-step loading is considered, the number n_c of vertical strips that have a crack (cohesive or LEFM) being increased one by one. After the iterations of the solution of each loading step converge, the vertical displacement u is evaluated from the compliance matrix. (If u rather than n_c were prescribed, the front of the crack in the radial direction would end arbitrarily between two nodes, which would slow down convergence and increase the scatter of results.)

In each loading step, one has a system of several hundred highly nonlinear equations. It is solved by the Levenberg-Marquardt iterative nonlinear optimization algorithm (Marquardt 1963), for which a standard library subroutine is used. The correct solution can be obtained with this algorithm only if a very good initial state can be supplied as the input. Fortunately, the present problem is of a special kind in which the solution can be traced in small steps. The solution obtained in each loading step can be used as a good initial estimate for the start of the optimization iterations in the next loading step.

The initiation of circumferential cracks (Fig. 1) from the faces of the radial cracks determines the maximum load. It is governed by the strength criterion (Fig. 1 bottom right). Therefore, the values of the radial normal stresses σ_{rr} on the top face of the plate are calculated for each node from the deflection curvature $w_{,rr}$ along the radial ray and the

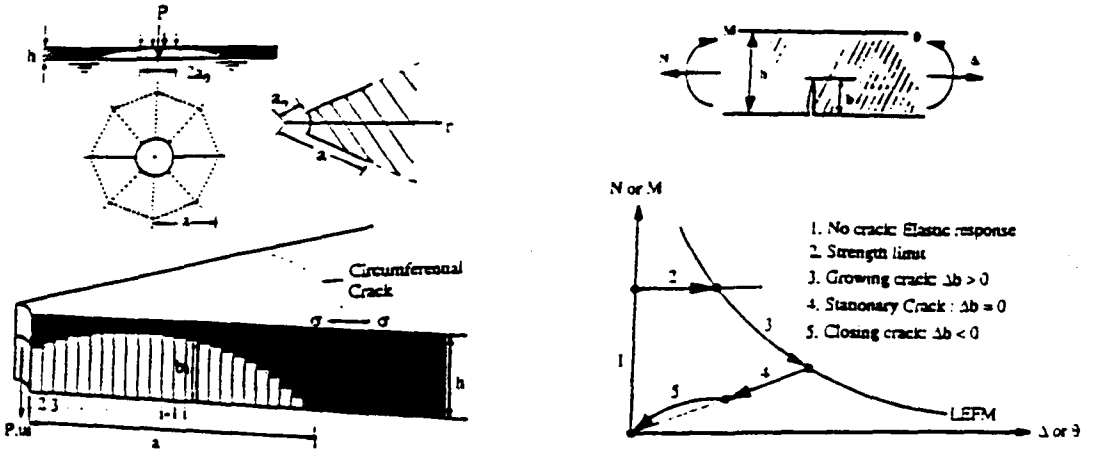

Figure 1. Top left: Vertical section and plan view of plate with cracks. Top right: Plate element with crack showing M, N, θ, Δ. Bottom left: Discretization of crack by vertical strips. Bottom right: Diagram of bending moment M or normal force N versus rotation θ or in-plane displacement Δ due to crack.

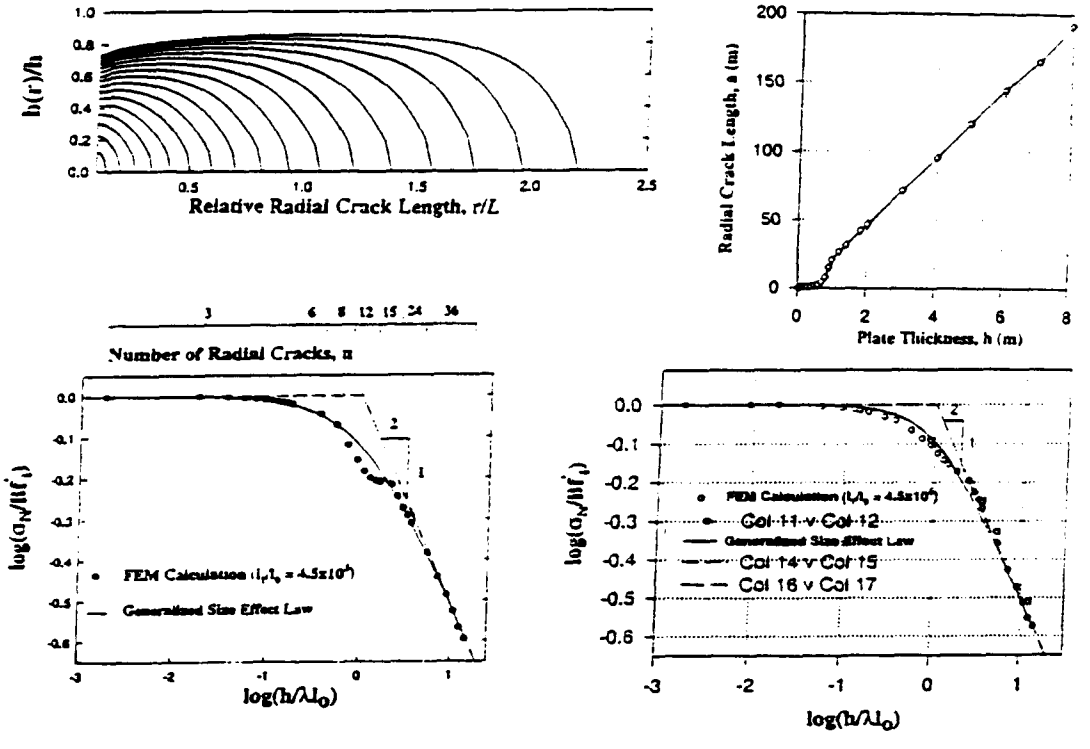

Figure 2. Top left: Calculated subsequent crack profiles (exaggerated vertical scale). Top right: Radial crack length versus plate thickness. Bottom: Calculated size effect for 6 cracks in a star pattern (right) and for variable number of cracks (left).

twist angle $w_{\theta r}$ along the θ arc (r = const.). These are approximated by a second-order finite difference formula from the nodal deflections w, using influence matrices calculated in advance.

Despite the fact that the maximum load is decided by the strength criterion, a size effect must be expected. The reason is that the failure occurs only as a consequence of radial crack growth, and that the attainment of a relative crack length at which the circumferential crack initiates is decided by the energy release criterion of fracture mechanics.

3 NUMERICAL RESULTS AND DISCUSSION

A schematic picture of the discretization of radial crack by vertical crack strips is shown in Fig. 1. The angle of the plate wedge between the radial cracks is considered as 60°. Because of symmetry, it suffices to analyze only a half wedge. A characteristic dimension of a floating plate in its plane is the flexural wavelength $L = (D/\rho)^{1/4}$ where ρ = specific weight of water. The ice plate is assumed to have a fixed support along a circle of radius $3L$, which is far enough to approximate an infinite plate. The circular hole along which the load P is applied has a finite radius $0.1L$, which avoids dealing with the stress singularity under a concentrated load. The typical ice characteristics are $f_t' = 0.2$ MPa, $\nu = 0.29$, $E = 1.0$ GPa, $K_c = 0.1$ MN m$^{-3/2}$ (Sanderson 1988). Figure 2 shows the typical calculated subsequent distributions of crack depth $b(r)$ with the radial coordinate r.

Size Effect. The size effect is understood as the dependence of the nominal strength $\sigma_N = P_{max}/h^2$ on h when geometrically similar structures are compared (P_{max} = maximum load). Failures governed by criteria expressed solely in terms of stresses or strains exhibit no size effect (Bažant1984; Bažant and Planas 1998).

The solution may be regarded as a functional relation among 8 variables: σ_N, h, G_f, f_t', E, ρ, ν, and a_0/L. However, the effect of the last is negligible, and the effect of E, ρ, and ν is fully characterized by flexural wavelength L. Therefore, the solution must be given by some function Π of only 5 variables, i.e. $\Pi(\sigma_N, h, G_f, f_t', L) = 0$. Buckingham's Π theorem of dimensional analysis (e.g., Barenblatt, 1979) states that the solution must be reducible to a function of N_π independent dimensionless variables where $N_\pi = N_{all} - N_{ind}$, N_{all} = 5 = number of all independent variables and N_{ind} = number of variables with independent physical dimensions, which are here only two, namely the length and force. So $N_\pi = 5 - 2 = 3$. Hence, the solution may be considered in the form:

$$\frac{\sigma_N}{f_t'} = \Phi\left(\frac{h}{l_0}, \frac{l_1}{l_0}\right) \qquad (2)$$

where Φ is some function and $l_0 = EG_f/f_t'^2 = K_c^2/f_t'^2$ and $l_1 = E/\rho \propto L^4/h^3$; $K_c = \sqrt{EG_f}$ = fracture toughness, l_0 = Irwin's (1958) characteristic size of the fracture process zone (also Hillerborg et al. 1976), and l_1 is a second independent length parameter. Note that the flexural wavelength $L = [l_1 h^3/12(1-\nu^2)]^{1/4}$.

We see that the elastic properties and specific weight of water influence the solution only through the ratio l_1/l_0. As for the fracture characteristics of ice, G_f and f_t', they influence the solution only through the value of l_0 but not individually. This means that the size effect curve of σ_N/f_t' versus h/l_0 has only one parameter, namely l_1/l_0.

The value of ρ is a constant. The values of G_f as well as f_t' for sea ice are functions of temperature, salinity and other factors, and display a large statistical scatter. The value of E has a much lower statistical scatter. The E-values measured by ultrasound range approximately from 4 GPa to 11 GPa. The effective value for static loading is much smaller because of creep (or rate effect). The value of $E = 1$ GPa (which is the same as considered by Evans, 1971) has been used.

For tensile strength f_t' the value of 0.5 MPa (Sanderson 1988, Dempsey et al. 1995) has been used. This value, however, is much less important than the fracture toughness K_c because the plastic zone at the crack tip is, at maximum load, very small. In small-scale tests, the K_c values range from 0.044 MPa m$^{-3/2}$ to 0.115 MN m$^{-3/2}$ (Sanderson 1988, p. 91, Urabe and Yoshitake 1981, and Weeks and Mellor 1984). The value $K_c = 0.1$ MN m$^{-3/2}$ (the same as considered by Bažant 1992b) was used. With $E = 1$ GPa, the corresponding value of fracture energy is $G_f = 10$ N/m, which was used by Bažant (1992b).

A higher value of fracture energy, namely G_f = 520 N/m (with $K_c = 2.1$ MN m$^{-3/2}$, $E \approx 8.8$ GPA), has been deduced from the recent large-scale in-situ size effect tests of Dempsey et al. (1995; see also Mulmule et al. 1995). With $f_t' \approx 2$ MPa, one gets $l_0 \approx 0.5$ m and $l_1/l_0 \approx 1.8 \times 10^6$. These are the effective values for the whole thickness of ice whose temperature varies from about −20° C on top to about −1° C in contact with sea water. The values from Dempsey et al.'s tests (Mulmule and Dempsey 1997), however, are pertinent to horizontal propagation of a long full-through vertical crack. In our problem the crack propagates mainly vertically, which is along the columnar ice crystals. This doubtless causes the fracture process zone to be smaller and thus the effective fracture energy lower.

Based on these considerations, the characteristic size of the fracture process zone is considered as l_0 = 0.25 m, with the ratio = 4.5x10^6. The size effect results for these parameters and for the failure mode

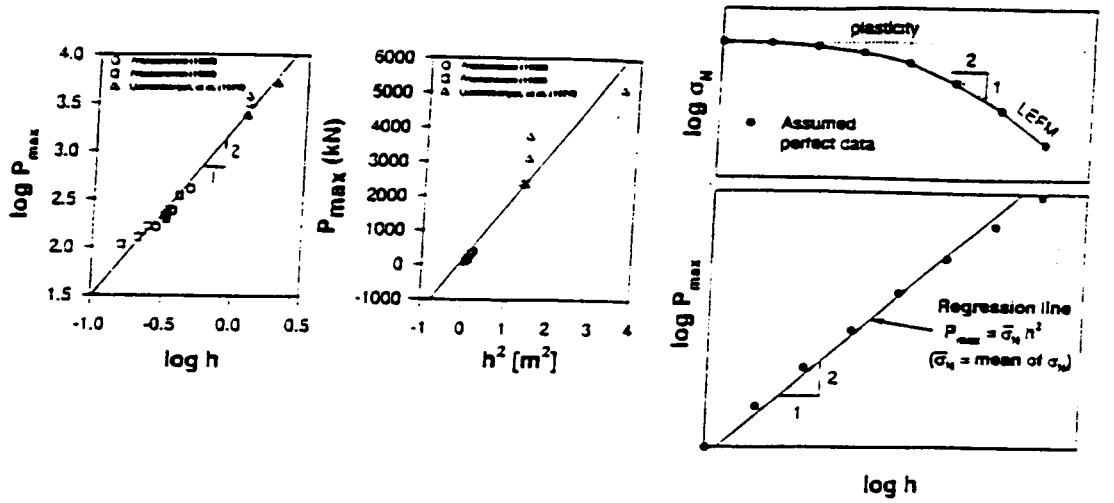

Figure 3. Left: Sodhi's (1995) way of plotting test data in terms of load P. Top right: Example of size effect data following Bažant's size effect law perfectly (no scater), in terms of σ_N. Bottom right: The same data replotted Sodhi's way, in terms of P.

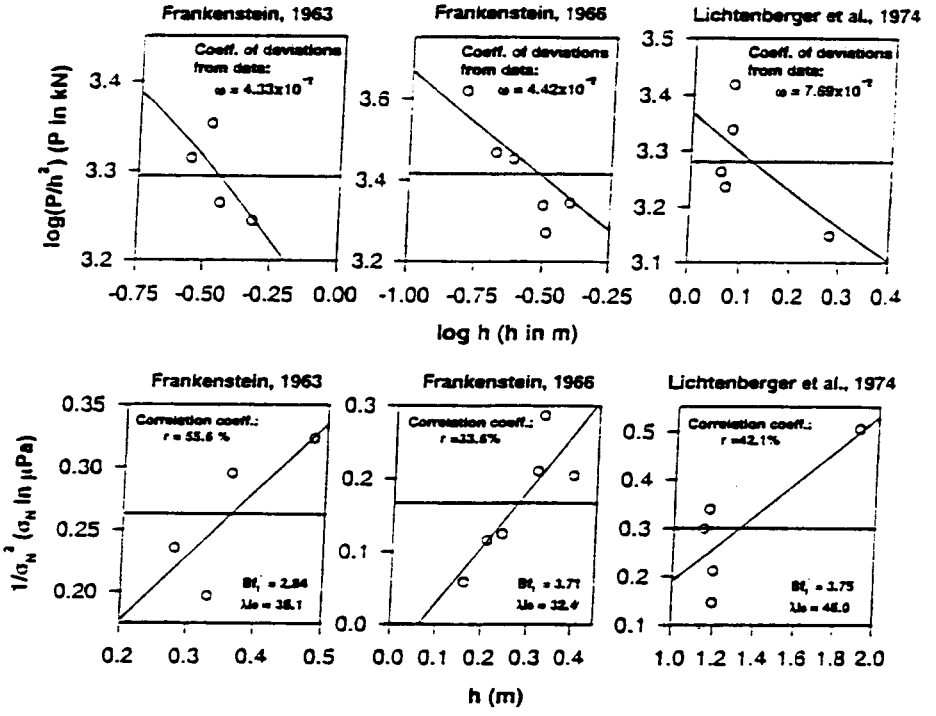

Figure 4. Size effect plots of existing test data (Frankenstein 1963, 1966; Lichtenberger et al. 1974) in terms of nominal strength σ_N.

with six cracks in a star pattern are shown by the data circles in the bi-logarithmic plot in Figure 2. The results for $l_1/l_0 = 3.9\text{x}10^4$ are shown in Figure 2 by the square points. The comparison shows that l_1/l_0 has only a minor effect. This is not surprising since l_1 and l_0 differ by several orders of magnitude, which means that they can hardly interact. So, the effect of l_1/l_0 can apparently be neglected.

The bump in the middle of the calculated data circles in Figure 2 (bottom plots) appears associated with the rapid rise in the ratio a/h seen in Figure 2 (top right), which occurs when h increases from 0.5 m to 1 m. For thicker plates, $a/h \approx 24$ at maximum load, which is a useful simple property ensuing from fracture mechanics. If a/h did not approach a constant for thick enough plates, the size effect plot would not approach an asymptote of slope $-1/2$. The reason that the size effect curve does have a horizontal asymptote for small sizes is not only the finite size of the fracture process zone (the zone in which $\sigma = f_t'$) but also, and perhaps mainly, the fact that initially, for small h, the crack length a does not increase as h is increased (Fig. 2, top right).

The dependence of the number of cracks n_c in the star pattern has also been studied. The angular spacing of the cracks was determined according to the stability analysis proposed by Bažant et al. (1979) (see also Bažant and Cedolin 1991, Sec. 12.6) and recently refined by Li and Bažant (1994) and Li, Hong and Bažant (1995). Taking the angular spacing as predicted in Li and Bažant (1994), the size effect shown in Figure 2 (bottom right) ensues. Comparison with the diagram on the left of Figure 2 shows that the number of cracks has only a minor effect.

Discussion of Size Effect. As is typical of quasibrittle fracture (e.g., Bažant and Planas 1998; Bažant 1984), the small-size asymptote of the calculated size effect plot (Fig. 2) is horizontal and corresponds to a solution according to plastic limit analysis (strength theory), whose applications to the penetration problem are reviewed by Kerr (1994); see also Sodhi (1995a,b, 1996). The present computations show that plastic limit analysis (strength theory) is a good enough approximation only for ice thicknesses up to about 0.2 m (assuming that $l_0 = 0.25$ m). At the same time, the σ_N values for the horizontal asymptote can scatter widely depending on the type of ice and the environmental conditions (air and water temperature). This may explain why no size effect (nor notch sensitivity) is observed in small-scale laboratory tests.

The large-size asymptote of the size effect plot, which has the slope of $-1/2$ corresponding to LEFM, is seen to be a good enough approximation for ice thicknesses over 1.0 m [in contrast to the case of full-through bending cracks (Bažant and Li 1994, Bažant 1992, Slepyan 1990), the slope is not $-3/8$]. The value of parameter λ_0 is chosen so that $h = \lambda_0 l_0$ represent the thickness at the intersection point of the two asymptotes. From the present numerical results, $\lambda_0 = 2.26$. The ratio $\beta = h/(\lambda_0 l_0)$ determined in this manner has been called the brittleness number (Bažant 1987, Bažant and Pfeiffer 1987; Bažant and Planas 1998). The limit $\beta \to \infty$ indicates the perfectly brittle response, i.e., LEFM, and the limit $\beta \to 0$ indicates the perfectly ductile (plastic) response.

By fitting of the present numerical results, spanning over four orders of magnitude of ice thickness, the following general prediction formula in the form of the generalized size effect law (Bažant 1985, 1987; Bažant and Pfeiffer 1987; Bažant and Planas 1998) results (see the curve in Fig. 2):

$$P_{max} = \sigma_N h^2, \quad \sigma_N = B f_t' \left[1 + (h/\lambda_0 l_0)^r\right]^{-1/2r} \quad (3)$$

with $B = 1.214$, $\lambda_0 = 2.55$, $m = 1/2$, $r = 1.55$ and $l_0 = 0.25$ m ($f_t' = 0.2$ MPa in Fig. 2). The form of this formula has been derived as the asymptotic matching between the large-size and small-size asymptotic expansions of the size effect (Bažant 1997a). Eq. (3) can be written as $Y = AX + C$ where $X = h^r$, $Y = (\sigma_N)^{-2r}$, $A = (B f_t')^{-2r}$, $C = 1/(\lambda_0 l_0 B f_t')^{2r}$. This means that, if r is known, the values of $B f_t'$ and $\lambda_0 l_0$ can be determined by linear regression. The regression is conducted for various trial values of r until the optimum r is found.

Comparison with Tests. The present results, showing the number of cracks n_c to increase with h, roughly agree with the available penetration experiments on lake ice (Frankenstein 1963, 1966, and Lichtenberger 1974). Sodhi (1995a,b, 1996) proposed a plasticity model, exhibiting no size effect, and claimed that the absence of size effect was confirmed by these data (Sodhi 1995a,b). However, this claim rested on a questionable statistical evaluation employing the plot of P_{max} versus h, as shown in Figure 3 (left). Indeed, this kind of plot visually suggests P_{max} to be approximately proportional to h^2, which would mean that σ_N is constant, free of size effect. Such a way of reasoning, however, is deceptive. The main reason is that, in this kind of plot, the size effect on σ_N is obscured by a superimposed much stronger deterministic variation of P_{max} as a linear function of h^2.

The deception of such a plot is illustrated in Figure 3 (right). In the diagram on top right, we assume hypothetical perfect data, conforming exactly to Bažant's size effect law. Then we plot the same data points in the graph of $\log P_{max}$ versus $\log h$ (Fig. 3, bottom right). According to Sodhi's opinion that there is no size effect, one would fit these data points with a straight regression line of slope 2, as shown. Visually, such a regression line seems quite acceptable, the deviations of the data points from the regression line appearing relatively small.

The comparison would look even more acceptable if we superimposed random scatter on the assumed data, as is the case in Sodhi's plot.

Another questionable aspect of Sodhi's (1995a,b) evaluation of the existing test data is that he correlated in the same diagram the test results from different test series while implying the ice properties to be the same. However, the ice properties in the two test series of Frankenstein (1963, 1966) and those of Lichtenberger et al. (1974) most likely differed, which means that the groups of data points for these tests in the plot in Figure 3 (left) could shift vertically relative to each other. Thus, what looks as a good agreement with the proportionality of P_{max} to h^2, would be lost by such vertical shifts. It might have been by chance that the differences among ice properties compensated for the size effect.

Because the size effect represents the deviation from the proportionality of P to h^2, a non-obfuscating way that can bring the size effect to light is to plot the values of nominal strength $\sigma_N = P/h^2$, rather than P, as a function of h, and make the plots separately for each test series, as shown in Figure 1. These plots lead to a conclusion different from Sodhi's—there is a clear size effect in each test series.

Furthermore, Figure 4 shows the linear regression plots of $1/\sigma_N^2$ versus h, in which the size effect law (3) is represented by the regression line. These plots permit determining the coefficients of variation, ω, of the slope of the regression line.

Neglected Phenomena. Due to temperature nonuniformity and diffusion of brine, the ice plate is not homogeneous. Its bottom, where the ice is near the melting point, is very soft and weak, while the top is cold and thus stiff and strong. The present approximate analysis must be interpreted in the sense of a certain effective ice thickness that gives about the same bending stiffness as the actual plate, and the values of K_f, f_t' and E must be interpreted as the equivalent effective properties throughout the thickness. Other simplifications are the neglect of the rate of loading or creep, and anisotropy. Furthermore, it could happen during loading that some of the radial cracks could suddenly start growing faster than others, breaking symmetry in the manner of a bifurcation of response path (Bažant and Cedolin 1991, Sec. 12.6).

4 CONCLUSIONS

1. The radial cracks extend only through part of the thickness of the plate.

2. A size effect exists for plates thicker than about 20 cm and plastic analysis is realistic only for plates thinner than that.

3. The size effect asymptotically approaches the law $\sigma_N \propto (\text{thickness})^{-1/2}$, characteristic of LEFM.

4. The number of radial cracks has only a small effect.

5. The existing limited field measurements of size effect agree with the present theory well.

6. Sodhi's opinion that there is no size effect is contradicted not only by the present theory but also by the existing field tests.

Acknowledgment: Financial support under grant N00014-91-J-1109 (monitored by Dr. Y. Rajapakse) from the Office of Naval Research to Northwestern University is gratefully acknowledged.

REFERENCES

Adamson, R.M., Dempsey, J.P., DeFranco, S.J., & Xie, Y. 1995. Large-Scale in-situ ice fracture experiments—Part I: Experimental Aspects. *ICE MECHANICS-1995* J.P. Dempsey & Y.D.S. Rajapakse (eds.), ASME AMD Vol. 207, 107–128.

Barenblatt, G.I. 1979. Similarity, self-similarity and intermediate asymptotics. *Consultants Bureau*, New York, NY.

Bažant, Z.P. 1984. Size effect in blunt fracture: concrete, rock, and metal. *J. of Engrg. Mech. ASCE*, 110, 518–535.

Bažant, Z.P. 1985. Fracture mechanics and strain-softening in concrete. Preprints, *U.S.-Japan Seminar on Finite Element Analysis of Reinforced Concrete Structures*, Tokyo, Vol. 1, 47–69.

Bažant, Z.P. 1987. Fracture energy of heterogeneous material and similitude. Preprints, *SEM-RILEM Int. Conf. on Fracture of Concrete and Rock* (held in Houston, Texas, June 1987), S. P. Shah & S. E. Swartz (eds.), publ. by SEM (Soc. for Exper. Mech.) 390–402.

Bažant, Z.P. 1992a. Large-scale fracture of sea ice plates. (Proc. *11th IAHR Ice Symposium*, Banff, Alberta), June, T.M. Hrudey (ed.), Dept. of Civil Engineering, University of Alberta, Edmonton, vol. 2, pp. 991–1005.

Bažant, Z.P. 1992b. Large scale thermal bending fracture of sea ice plate. *J. Geophysical Research Oceans*, Vol. 97 (C11), 17739–17751.

Bažant, Z.P. 1993. Scaling laws in mechanics of failure. *J. Engrg. Mech. ASME*, 119 (9), 1828–1844.

Bažant, Z.P. 1997a. Scaling of quasibrittle fracture: asymptotic analysis. *Int. J. of Fracture*, 83 (1), 19–40.

Bažant, Z.P. 1997. Scaling of quasibrittle fracture: Hypotheses of invasive and lacunar fractality, their critique and Weibull connection. *Int. J. of Fracture* 83 (1), 41–65.

Bažant, Z.P., & Cedolin, L. 1991. *Stability of structures: Elastic, Inelastic, Fracture and Damage Theories*, Oxford University Press, New York.

Bažant, Z.P., & Chen, E.-P. (1997). Scaling of structural failure. *Applied Mechanics Reviews* ASME 50 (10), 593–627.

Bažant, Z.P., & Gettu, R. 1991. Size effects in the fracture of quasi-brittle materials. in *Cold Regions Engineering* (Proc., *6th ASCE International Specialty*

Conference, held in Hanover, NH, Feb. 1991), D.S. Sodhi (ed.), ASCE, New York, 595–604.

Bažant, Z.P., & Kim, J.-K. 1985. Fracture theory for nonhomogeneous brittle materials with application to ice. Proc. *ASCE Nat. Conf. on Civil Engineering in the Arctic Offshore — ARCTIC 85*, San Francisco, L. F. Bennett (ed.), ASCE, New York, 917–930.

Bažant, Z.P., Kim, J.J., & Li, Y.-N. 1995. Part-through bending cracks in sea ice plates: Mathematical modeling. *ICE MECHANICS-1995*, J.P. Dempsey & Y. Rajapakse (eds.), ASME AMD-Vol. 207, 97–105.

Bažant, Z.P., & Kim, J.J.H. 1998. Size Effect in Penetration of Sea Ice. *J. of Eng. Mech.* ASCE; in press.

Bažant, Z.P., & Li, Y.-N. 1994a. Penetration fracture of sea ice plate: Simplified analysis and size effect. *J. of Engrg. Mech. ASCE* 120 (6), 1304–1321.

Bažant, Z.P., & Li, Y.-N. 1994b. Penetration through floating sea ice plate and size effect: simplified fracture analysis. *J. Engng. Mech. ASCE*, 120 (7), 1304–1321.

Bažant, Z.P., Ohtsubo, R., & Aoh, K. 1979. Stability and post-critical growth of a system of cooling and shrinkage cracks. *Int. J. of Fracture*, 15, 443–456.

Bažant, Z.P., & Pfeiffer, P. A. 1987. Determination of fracture energy from size effect and brittleness number. *ACI Materials Jour.*, 84, 463–480.

Bažant, Z.P., & Planas J., 1998. Fracture and size effect in concrete and other quasibrittle materials. CRC Press, Boca Raton, Florida.

Bernstein, S. 1929. The railway ice crossing (in Russian), *Trudy Nauchno-Technicheskogo Komiteta Narodnogo Komissariata Putei*, Soobshchenniya, Vol. 84, Moscow.

DeFranco, S.J., & Dempsey, J.P. 1990. Crack growth stability in S2 ice. *Proc., 10th Int. IAHR Symp. on Ice*, 168–181.

Dempsey, J.P. 1989. The fracture toughness of sea ice. *Ice/Structure Interaction*, S. Jones et al., eds., Springer Verlag, New York 109–145.

Dempsey, J.P. 1990. Notch sensitivity of ice. *Proc., First Materials Engineering Congress*, Vol. 2, ASCE, New York, 1124–1133.

Dempsey, J.P., Adamson, R.M., & Mulmule, S.V. 1995. Large-scale in-situ fracture of ice. *Proceedings of FRAMCOS-2*, edited by Wittmann, F.H., AEDIFICATIO Publishers, D-79104 Freiburg, 1995.

Dempsey, J.P. 1996. Scale effects on the fracture of ice. *The Johannes Weertmann Symposium*, R.J. Arsenault et al, Editors, The Minerals, Metals & Materials Society (TMS), Warrendale, Pennsylvania, 351–361.

Dempsey, J.P., Slepyan, L.I., & Shekhtman, I.I. 1995. Radial cracking with closure. *Int. J. of Fracture*, 73 (3), 233–261.

Frankenstein, E.G. 1963. Load test data for lake ice sheet. *Technical Report 89*, U.S. Army Cold Regions Research and Engineering Laboratory, Hanover, New Hampshire.

Frankenstein, E.G. 1966. Strength of ice sheets. *Proc., Conf. on Ice Pressures against Struct.; Tech. Memor. No. 92, NRCC No. 9851*, Laval University, Quebec, National Research Council of Canada, Canada, 79–87.

Hillerborg, A., Modéer, M., & Petersson, P.E., 1976. Analysis of crack formation and crack growth in concrete by means of fracture mechanics and finite elements. *Cem. & Concrete Res.* 6, 773–782.

Kerr, A.D. 1975. The bearing capacity of floating ice plates subjected to static or quasi-static loads—A critical survey. *Res. Report 333*, U.S. Army Cold Regions Res. & Engrg. Laboratory, Hanover, NH.

Kerr, A.D. 1996. Bearing capacity of floating ice covers subjected to static, moving, and oscillatory loads. *Appl. Mech. Rev., ASME Reprint*, 49 (11), 463–476.

Kuo, C.H., Keer, L.M., & Cordes, R.D. 1995. A note on the line spring solution for a part-through crack. *Int. J. of Fracture* 72, 191–195.

Li, Y.-N., & Bažant, Z.P. 1994. Penetration fracture of sea ice plate: 2D analysis and size effect. *J. of Engrg. Mech. ASCE* 120 (7), 1481–1498.

Li, Y.-N., Hong, A.N., & Bažant, Z.P. 1995. Initiation of parallel cracks from surface of elastic half-plane. *Int. J. of Fracture* 69, 357–369.

Lichtenberger, G.J., Jones, J.W., Stegall, R.D., & Zadow, D.W. 1974). Static ice loading tests Resolute Bay—Winter 1973/74. *APOA Project No. 64, Rep. No. 745B-74-14, (CREEL Bib. No. 34-3095j*, Sunoco Sci. & Technol., Rechardson, Texas.

Marquardt, D.W. 1963. An algorithm for least-squares estimation of nonlinear parameters. *J. Soc. Industr. Appl. Math.* 11, 431–441.

Mulmule, S.V., & Dempsey, J.P. 1997. Stress-separation curves for saline ice using fictitious crack model. *J. of Engrg. Mech. ASCE* 123 (8), 870–877.

Mulmule, S.V., Dempsey, J.P., & Adamson, R.M. 1995. Large-scale in-situ ice fracture experiments—Part II: Modeling apects, *ICE MECHANICS-1995*, J.P. Dempsey & Y. Rajapakse (eds.), ASME AMD-Vol. 207, 129–146.

Nevel, D.E. 1958. The theory of narrow infinite wedge on an elastic foundation. *Transactions, Engineering Institute of Canada*, 2(3)

Rice, J.R. & Levy, N. 1972. The part-through surface crack in an elastic plate. *J. Appl. Mech. ASME*, 39, 185–194.

Sanderson, T.J.O. 1988. *Ice Mechanics: Risks to Offshore Structures*, Graham & Trotman Ltd., London.

Slepyan, L.I. 1990. Modeling of fracture of sheet ice. *Mechanics of Solids* (transl. of Izv. AN SSSR Mekhanika Tverdoga Tela), 155–161.

Sodhi, D.S. 1995a. Breakthrough loads of floating ice sheets. *J. Cold Regions Engrg. ASCE*, 9 (1), 4–20.

Sodhi, D.S. 1995b. Wedging action during vertical penetration of floating ice sheets. *ICE MECHANICS-1995*, J.P. Dempsey & Y. Rajapakse (eds.), ASME AMD-Vol. 207, 65–80.

Sodhi, D.S. 1996. Deflection analysis of radially cracked floating ice sheets. *17th Int. Conf. OMAE Proceedings*, Book No. G00954, 1996, 97–101.

Urabe, N., Yoshitake, A. 1981. Strain-rate dependent fracture Ztoughness (K_{Ic}) of pure ice and sea ice., *Proc. IAHR 81*, Vol. 2, 410–420.

Weeks, W.F., & Mellor, M. 1984. Mechanical properties of ice in the Arctic seas. in *Arctic Technology & Policy*, I. Dyer & C. Chryssostomidis (eds.), Hemisphere, Washington, D.C., 235-259.